ARPES spectra from cuprates in the bond-ordered, bond-centred stripe phase

2006 J. Phys.: Condens. Matter 18 9749

(http://iopscience.iop.org/0953-8984/18/42/017)

INSTITUTE OF PHYSICS PUBLISHING JOURNAL OF PHYSICS: CONDENSED MATTER

J. Phys.: Condens. Matter **18** (2006) 9749–9770 doi:10.1088/0953-8984/18/42/017

ARPES spectra from cuprates in the bond-ordered, bond-centred stripe phase

P Wróbel[1,2], **A Maciąg**[2] **and R Eder**[3]

[1] Max Planck Institute for the Physics of Complex Systems, D-01187 Dresden, Germany
[2] Institute for Low Temperature and Structure Research, PO Box 1410, 50-950 Wrocław 2, Poland
[3] Forschungszentrum Karlsruhe, IFP, PO Box 3640, D-76021 Karlsruhe, Germany

E-mail: p.wrobel@int.pan.wroc.pl

Received 21 April 2006, in final form 31 August 2006
Published 6 October 2006
Online at stacks.iop.org/JPhysCM/18/9749

Abstract

The electronic structure and the single-particle spectral density of a stripe array formed by ladder-like domain walls (DWs) and by antiferromagnetic (AF) domains of width two lattice spacings are computed and compared with angle-resolved photoemission spectroscopy (ARPES) spectra from some doped cuprates belonging to the 214 family of compounds. We assume that bond order is formed on legs in DWs and that the phase of the sublattice magnetization changes by π across each DW. The intensity map plotted in the frame of reference momentum–energy reproduces quite well the ARPES spectra of Nd-doped $La_{2-x}Sr_xCuO_4$ (LSCO) systems obtained at the doping level of 15%. We consider this agreement as an argument for a scenario of coexisting bond-ordered regions and AF regions in the stripe phase of moderately doped cuprates.

(Some figures in this article are in colour only in the electronic version)

1. Introduction

A tendency towards spin and charge ordering in cuprates has been seen in the results of several neutron scattering experiments [1]. Low-frequency spin fluctuations observed by many groups at incommensurate wavevectors as relatively sharp peeks in the magnetic structure factor [2–4] have been interpreted as being due to stripe fluctuations [5]. The anisotropy of resistivity [6] also points at stripe formation. Stripes appear to influence phonon-mediated heat transport [7]. Furthermore, measurements performed by means of NMR and NQR techniques demonstrate the emergence of slow spin fluctuations whose appearance is correlated with pinning of charge modulations [8]. The distribution of nearest-neighbour bond lengths deduced from neutron powder diffraction data [9, 10] and measured by means of extended x-ray-absorption fine structure spectroscopy [11] also seems to basically agree with expectations based on a scenario

of lattice response to local charge-stripe order. Moreover, an indication of stripe order may by found by analysing the shape of ARPES spectra and their evolution with doping. For example, it is natural to expect the Fermi surface to be flat in the stripe phase in the antinodal region, near the vectors $(\pm\pi, 0)$ and $(0, \pm\pi)$ [5]. In addition, quasi-one-dimensionality of the system should bring about the depletion of spectral weight in the nodal regions, near the Brillouin zone diagonals. Much research has been done to check if these hypotheses are true [5, 12–16]. It seems that some general structure of spectra may be definitely attributed to an underlying quasi-one-dimensional electronic structure [17–27].

In this paper we will concentrate on doped LSCO compounds, slightly above the doping level 1/8 at which, it is believed, a tendency towards nanoscale phase separation seems to be evident in the ARPES results [13, 16, 28]. Patches with high intensity may be seen in antinodal regions in ARPES intensity maps obtained by integrating the spectra from 15% doped $La_{2-x-y}Nd_ySr_xCuO_4$ (Nd-LSCO) [14]. The integration is performed in the 30 meV window at the Fermi energy. Contrary to some predictions, appreciable spectral weight is detected at the Fermi energy in nodal regions. A similar pattern of the spectral density at the Fermi energy was predicted by a phenomenological theory of disordered charge stripes and antiphase spin domains [29]. Unfortunately, this ingenious theory does not discuss the origin of renormalized hopping terms in the effective one-body Hamiltonian and does not explain the relation of the parameter renormalization with the underlying magnetic structure. The evolution of the spectral weight as a function of doping has been analysed for the stripe phase by means of the cluster perturbation technique (CPT) in the framework of the microscopic t–J and Hubbard models [26]. This theory captures quite well the general trend of this development. Nevertheless, it seems that the spectral weight maps derived within this approach for the doping level at and above 12.5% do not show continuous well developed high-intensity straight patches bridging antinodal regions. As we have already mentioned, such structures are experimentally seen in nodal regions [14]. The remarks made above seem to suggest that some understanding of the relation between the single particle spectral weight of Nd-LSCO at the filling level about 1/8 and the formation of the stripe phase is missing. A phase which we may expect to emerge in a natural way in weakly doped antiferromagnets is a bond-ordered state [30]. Recently, an exact diagonalization of the t–J model (tJM) at a finite cluster has been performed to study stripe formation. It has been shown that the cluster-geometry change, from the standard tilted square form of the 20-site cluster to the rectangular form of the 5×4 cluster, induces the formation of a ground state with pronounced stripe-like charge inhomogeneities [31]. The distribution of peaks in the single-particle spectral weight, which has been calculated by means of the same method [32], resembles experimental ARPES spectra from $La_{1.28}Nd_{0.6}Sr_{0.12}CuO_4$ [13]. In particular, the theory captures quite well the strong dispersion along the $(0, 0)$–$(\pi, 0)$ line. The distribution of quasiparticle peaks in the single-particle spectrum obtained by means of the exact diagonalization is in good agreement with the results of an additional calculation performed by means of a different method, the bond operator theory. Unfortunately, neither the numerical approach nor the analytical method reproduce the flattening of the experimental band near the point $(\pi, 0)$ and both of them fail to explain the emergence of the spectral weight at the nodal region, in the form of a straight patch which is observed at the Fermi energy in the experiments. Another analysis of the spectral weight in doped antiferromagnets, based on the exact diagonalization of a small cluster, concerns the tJM with inhomogeneous terms locally breaking the translational invariance and the spin-rotational $SU(2)$ symmetry [23]. The pattern of the integrated spectral weight at the Fermi energy obtained by means of this method resembles, to certain extent, ARPES spectra from Nd-LSCO at the doping level 12%. Nevertheless, that pattern does not show enhanced intensity at nodal regions either. The enhancement observed in experiments is the manifestation of remnant two-dimensionality in

the stripe system. Thus, the analysis based on adding terms breaking the $SU(2)$ symmetry seems do not account for the shape of ARPES spectra from Nd-LSCO or LSCO at a doping level slightly higher than $1/8$ either.

The results of inelastic neutron scattering (INS) experiments indicate that pronounced AF correlations exist in the stripe phase [3]. On the other hand, the relevance of bond order has been recently demonstrated by means of the same experimental method [33]. In a recent work [34] we have suggested that the coexistence of bond order with long-range AF order may take place in the stripe phase. The scenario of nanoscale phase separation is realized by means of this coexistence. In the framework of this concept we have shown that above the doping level $1/8$, when the distance between stripe axes is four lattice spacings, a bond-centred stripe with bond order inside stripes is more stable than a site-centred stripe. It is also known about the site-centred stripe that it is more stable than a homogeneous system of holes created in the homogeneous antiferromagnet [20, 35]. The latter piece of information gives rise to the final conclusion that bond order may exist with AF order in the stripe phase of cuprates at doping levels above $1/8$. The mechanism of that coexistence is based on lowering the kinetic energy of holes moving freely in hole-rich stripes which are formed as two-leg ladder-like DWs between AF hole-poor domains in which the exchange energy decreases [34].

In the next section, in the framework of a scenario for nanoscale phase separation and coexistence of AF long-range order with bond order, we will derive an effective tight-binding Hamiltonian describing a quasiparticle propagating in such a spin background. Next, we will calculate the part of the spectral function which is accessible to measurements in photoemission experiments. Finally we will discuss the calculation results. They seem to show characteristic features which may be seen in ARPES spectra of Nd-LSCO slightly above the doping level $1/8$.

2. Band structure of a stripe system with coexisting bond and AF orders

The tJM in the framework of which we perform the calculation is

$$H = -\sum_{i,j} t_{ij} c^{\dagger}_{i,\sigma} c_{j,\sigma} + J \sum_{\langle i,j \rangle} \left(\mathbf{S}_i \mathbf{S}_j - \frac{n_i n_j}{4} \right). \tag{1}$$

The states in which any site is doubly occupied have been excluded by definition from the Hilbert space in which that model acts. $\langle i, j \rangle$ represents a pair of nearest-neighbour (NN) sites. $\vec{S}_i$ and n_i denote the operators of electron spin and density at site i respectively. The hopping matrix element between NN sites in the square lattice on which the tJM is defined is t. t' is the hopping matrix element between second-NN sites, and t'' is the hopping matrix element between third-NN sites. The rest of the hopping integrals $t_{i,j}$ vanish. We concentrate on the doping level about $1/8$, at which the distance between axes of nearest stripes is four lattice spacings and AF correlations seem to be of long range [3]. Our previous analysis has provided convincing arguments that in such a case the stripe takes the form of a two-leg ladder-like DW which separates hole-poor AF domains [34]. The phase of sublattice magnetization in domains changes by π across a DW. Each DW is bond ordered. Singlets are formed on legs of the ladder-like DW. The underlying spin structure of the stripe system at the doping level about $1/8$ has been presented in figure 1. A natural question arises: what is mechanism which gives rise to long-range AF correlations, if AF domains are separated by DWs which consist of singlets [36]? The structure depicted in figure 1 emerges in the presence of doped holes only. The creation of a hole gives rise to the appearance of an uncompensated spin in the DW. This spin may be parallel or antiparallel to a nearest spin in the neighbour domain. The weight of states in which these spins are antiparallel, figures 2(a), (b), is higher, because such

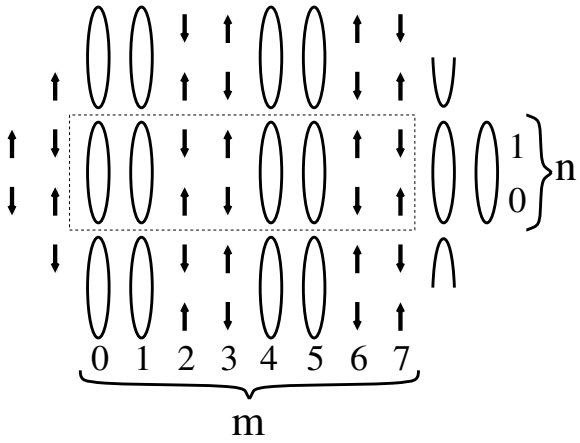

Figure 1. Elementary cell of the underlying spin structure assumed in the calculation (inside the dashed rectangle). Ovals represent singlets.

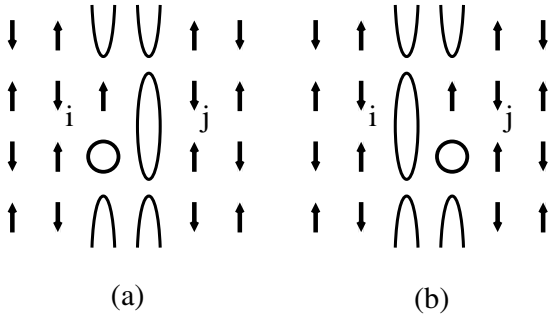

Figure 2. The mechanism which gives rise to FM coupling between nearest spins that belong to different domains. These spins would belong to the same AF sublattice if the system were homogeneously ordered.

a configuration is preferred by AF coupling between NN sites. States depicted by figures 2(a) and (b) are coupled by the hopping term in the Hamiltonian. Since their weight is higher than the weight of states in which an uncompensated spin in the DW and the nearest spin in the domain are parallel, the hopping term which transforms the state depicted by figure 2(a) into the state depicted by figure 2(b) mediates effective ferromagnetic (FM) coupling between sites i and j. Some quantum fluctuations will be present in the underlying spin background of the stripe system. They may take the form of triplet excitations on bonds in DWs and multimagnon excitations in domains. Figure 4 in the previous work [34] contains some examples of quantum fluctuations in the spin background. They contribute a lot to the energy of the system. On the other hand, it seems that quantum fluctuations merely renormalize the shape of quasiparticle dispersion for a given spin background and do not give rise to qualitative changes. This has been demonstrated in the case of a hole propagating in the AF spin background [37], as well as in the case of bond-ordered two-leg ladders [38, 39] and bond-ordered two-dimensional (2D) systems [32]. When it is necessary we will take into account the influence of quantum fluctuations on the distribution of spectral weight. A scenario which underlies the calculation which we are going to outline next is based on the assumption that hole motion inside ladder-like DWs is governed by the exchange of positions between a hole–fermion pair on a bond and a singlet on a nearby bond [38]. This exchange is mediated by the hopping terms in the initial Hamiltonian (1). We also assume that a hole propagates in the AF spin background as a spin polaron [40]. In the calculation we take into account a simplest form of coupling which moves a hole between a bond-ordered DW and an AF domain. This form of coupling originates in the hopping term of the initial Hamiltonian. During the construction of an effective

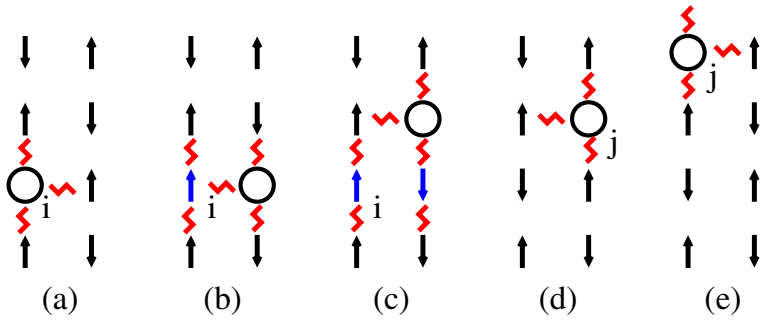

Figure 3. Graphical representation of some states involved in the process of hole propagation inside an AF domain. Zig-zag lines represent 'broken-bonds'. Contributions from them to Ising energy are higher by $J/2$ than the contributions from bonds occupied by two antiparallel spins.

Hamiltonian which describes the motion of a quasiparticle in the underlying spin background, some formulae will be useful. They are presented in the appendix.

We begin the derivation of the effective Hamiltonian describing hole propagation in the spin background depicted by figure 1 by outlining the mechanism of hole propagation inside an AF domain. A hole created and moving in the Néel background shifts spins between different sublattices and creates defects in the AF structure; see figures 3(a)–(c). Such a process gives rise to an increase of the Ising energy. This rise is roughly speaking proportional to the length of a path along which the hole has travelled, which means that a tendency towards hole confinement appears [41]. In order to take into account such a tendency we will analyse the hole motion in the framework of a basis which consists of states representing holes confined in the AF background by linear defects (strings) left behind by moving holes on their way. We call these states spin polarons. A wavefunction representing a confined spin polaron at a site i in an AF domain is a combination of states which are created from the state $c_{i,\uparrow(\downarrow)}|N\rangle$ by the NN hopping term when a hole created at the site i starts to move inside the domain,

$$|\Psi_i\rangle = \sum_{\mathcal{P}_i} \alpha_{l(\mathcal{P}_i)}|\mathcal{P}_i\rangle; \tag{2}$$

$|N\rangle$ is the Néel state in the domain, and $|\mathcal{P}_i\rangle$ denotes a state obtained by hopping along a path $\mathcal{P}_i$ of a hole created at the site i. $\alpha_{l(\mathcal{P}_i)}$ is the amplitude of this state. We have assumed for simplicity that $\alpha_{l(\mathcal{P}_i)}$ depends solely on the length $l(\mathcal{P}_i)$ of the path $\mathcal{P}_i$. The length of a path or of a string state is defined as the number of hops needed to form a given string state from a state representing a hole created in the AF spin medium. At the first stage of the analysis we take into account only the hopping between NN sites because $t \gg J, t', t''$. Processes related to hopping between further neighbours and processes related to swapping antiparallel spins by the transversal term in the exchange interaction will be considered later as a perturbation. A hole moving inside a domain may make its first step in $(z-1)$ directions. $z = 4$ is the coordination number of the square lattice. There are in principle $(z-2)$ direction choices of each next hop, if the hole moves without retracing inside the domain. On the full square lattice there are z choices for the direction of the first step and $(z-1)$ for the direction of further hops during the non-retractable motion. These number gets reduced by one for the domain formed by two chains of sites. Thus if we neglect some details, as for example path crossing, we may write

$$\langle\Psi_i|\Psi_i\rangle = \alpha_0^2 + (z-1)\sum_{\mu=1}(z-2)^{\mu-1}\alpha_\mu^2. \tag{3}$$

Each prefactor in (3) at the square α_μ^2 represents the number of different paths with the length μ. We calculate the energy of the spin polaron state $|\Psi_i\rangle$, ε_1 which is given by the expectation value of a trial Hamiltonian H_0, $\langle\Psi_i|H_0|\Psi_i\rangle$ with the assumption that the motion of a hole which has started from the site i is restricted to the interior of the domain and that the contribution from the interaction term is restricted to the Ising part $\sum_{\langle i,j\rangle}(S_i^z S_j^z - \frac{n_i n_j}{4})$,

$$\langle\Psi_i|H_0|\Psi_i\rangle = \left[3\alpha_0^2 + (z-1)\sum_{\mu=1}(z-\mu)^{\mu-1}(4+\mu)\alpha_\mu^2\right]\frac{J}{2} + 2(z-1)\sum_{\mu=0}(z-2)^\mu\alpha_\mu\alpha_{\mu+1}t. \tag{4}$$

The first term in (4) basically counts the number of 'broken bonds', that are not occupied by a pair of antiparallel spins, in which case the Ising contribution to the energy of that bond is higher by $J/2$ than in the case if it were occupied by a pair of antiparallel spins. The second term in (4) is the contribution from the hopping operator to the spin polaron energy. The prefactors appearing in this term represent the number of paths with a given length multiplied by the number of directions in which these paths may be extended. The appearance of the factor 2 is related to the fact that the hopping which couples paths of length μ and $\mu+1$ may take place forth and back. The values of parameters α_μ can be found by minimizing $\langle\Psi_i|H|\Psi_i\rangle$ under the constraint $\langle\Psi_i|\Psi_i\rangle = 1$. After we have constructed spin polarons which are formed in AF domains we are able to present the full basis of single-particle states. The underlying spin background which has been presented in figure 1 plays the role of the vacuum $|\Omega\rangle$ for hole-like quasiparticles which propagate in this background. $|\Omega\rangle$ has been obtained by acting on the absolute vacuum $|0\rangle$, in which no particles are present, with a product of operators like $s_{LU}^\dagger$ creating singlets on bonds connecting sites L and U and operators $c_{i\sigma}^\dagger$ creating spins in domains according to the pattern shown in figure 1. New fermionic operators $h_{i\sigma}^\dagger$ create single-particle positively charged hole-like states from the vacuum for holes $|\Omega\rangle$. The action of the operator $h_{L\sigma}^\dagger(h_{U\sigma}^\dagger)$ on $|\Omega\rangle$, where the site $L(U)$ belongs to a ladder-like DW, exchanges the operator $s_{LU}^\dagger$ in the product defining $|\Omega\rangle$ by the operator $c_{U\sigma}^\dagger(c_{L\sigma}^\dagger)$, which means that instead of a singlet on the bond connecting sites L and U there is a hole on the site $L(U)$ and spin σ on the site $U(L)$. The action of the operator $h_{i\sigma}^\dagger$ on a site i which belongs to an AF domain creates a spin polaron $|\Psi_i\rangle$ in that domain. The spin polaron is a combination of some states, the amplitudes of which are given by prefactors α_μ. These states include $c_{i\bar{\sigma}}|\Omega\rangle$ and states obtained by applying consecutively the NN inside-domain hopping term to the state $c_{i\bar{\sigma}}|\Omega\rangle$. A label which we will use to mark the fermionic operator creating either a bond hole or a hole-like spin polaron at a given site is $\binom{m,n}{i,j}$. m refers to the column number labelling the position of the unitary cell to which belongs the site where the hole-like particle has been created, n refers to the row number labelling the position of the unitary cell, and i (column), j (row) are indices representing the position of that site inside that unitary cell. i and j run from 0 to 7 and from 0 to 1, respectively. Now we start to explain with some details the origin of contributions to the effective Hamiltonian for a single quasiparticle propagating in the spin background depicted by figure 1 which is an exemplification of coexistence between AF and bond orders. We concentrate on the case of a spin-up quasiparticle. Within the approximation which we use, we may assume that operators $h_{i\uparrow}^\dagger$ create in the vacuum $|\Omega\rangle$ eigenstates of the unperturbed Hamiltonian H_0, which may be represented by the following formula:

$$H_0 = \sum_{\langle i,j\rangle} S_i S_j - t\sum_{\langle i',j'\rangle} c_{i'\sigma}^\dagger c_{j'\sigma} + J\sum_{\langle i',j'\rangle}\left(S_{i'}^z S_{j'}^z - \frac{n_{i'}n_{j'}}{4}\right) \tag{5}$$

where $\langle i, j\rangle$ are pairs of sites on which singlets depicted in figure 1 have been formed and $\langle i', j'\rangle$ are pairs of NN sites belonging to AF domains. The action of H_0 is restricted to the space containing states in which none of the sites is doubly occupied. This Hamiltonian contains the Ising part of the exchange energy of links inside domains. It also drives hole hopping between NN sites inside each domain. Since all matrix elements which may give rise to deconfinement of a hole have been by definition removed from H_0, polaron states $|\Psi_i\rangle$ are its eigenstates. Processes which bring about deconfinement of holes will be treated at the latter stage of the calculation as a perturbation. The matrix elements of the representation (5) for the unperturbed Hamiltonian H_0 and the matrix elements of the true trial Hamiltonian, eigenstates of which are localized spin polaron states (2), are actually different in some cases for states representing longer strings. Within our approximation in which details of longer strings are neglected those differences are either irrelevant because they appear for longer paths or we systematically take them into account. The exchange energy of sites forming bonds occupied by singlets in figure 1 are the only contribution to the Hamiltonian H_0 from DWs. Terms in the Hamiltonian of the tJM which couple a site belonging to a ladder-like DW with a site belonging to a domain do not contribute to H_0. Thus, it is clear that within our approximation the vacuum state $|\Omega\rangle$ and the single particle states $h^{\dagger}_{i\sigma}|\Omega\rangle$ are eigenstates of H_0 for i located both in domains and in DWs. Within the lowest-order approximation the on-site energy of a quasiparticle with spin up created at the site $\binom{m,n}{0,1}$ which belongs to a DW is $2J$. From now on, the reference value of the energy is the energy of the vacuum state $|\Omega\rangle$. The contribution from a destroyed singlet to the on-site energy of a hole-like quasiparticle created at the site $\binom{m,n}{0,1}$ is $(3/4)J$. A hole-like quasiparticle occupying the site $\binom{m,n}{0,1}$ with spin up is by definition the same as a single fermion with spin up which occupies the site $\binom{m,n}{0,0}$ belonging to the bond $\binom{m,n}{0,0}$–$\binom{m,n}{0,1}$. Since spins on the sites $\binom{m,n}{0,0}$ and $\binom{m-1,n}{7,0}$ are in this case parallel, the lowest-order contribution to the exchange energy of the bond between these two sites additionally increases by $J/4$ compared to the contribution from this bond in the vacuum state $|\Omega\rangle$. In the presence of a hole, the contribution from the potential term $-\sum_{\langle i,j\rangle} n_i n_j/4$ in the initial Hamiltonian of the tJM is higher by J. By adding all partial contributions we get the value $2J$ of the total on-site energy of the spin-up quasiparticle at the site $\binom{m,n}{0,1}$. Spin-up quasiparticles created in DWs at all sites which are NNs of sites in domains occupied by spins pointing down, have the same on-site energy.

Finally we deduce that in the effective single-particle Hamiltonian representing the propagation of a quasiparticle there appears a term

$$\delta_1 H_{\mathrm{eff}} = 2J \sum_{m,n} \left[h^{\dagger}_{\binom{m,n}{0,1}\uparrow} h_{\binom{m,n}{0,1}\uparrow} + h^{\dagger}_{\binom{m,n}{1,1}\uparrow} h_{\binom{m,n}{1,1}\uparrow} + h^{\dagger}_{\binom{m,n}{4,0}\uparrow} h_{\binom{m,n}{4,0}\uparrow} + h^{\dagger}_{\binom{m,n}{5,0}\uparrow} h_{\binom{m,n}{5,0}\uparrow} \right]. \tag{6}$$

The fermionic operators $h^{\dagger}_{\binom{m,n}{i,j}}$ and $h_{\binom{m,n}{i,j}}$ transform the underlying vacuum $|\Omega\rangle$ into the single-particle state representing a hole created in a DW and the single-particle state into $|\Omega\rangle$, respectively. The notation for indices which we use seems not to be very short, but such a form of it is basically unavoidable because the elementary cell of the underlying spin background, figure 1, is rather big. That notation also helps to trace easily at the map, which is figure 1, the results of hopping events mediated by the Hamiltonian H_{eff}. An analogous term will appear in the Hamiltonian representing a propagating spin-down quasiparticle, but with a different set of indices labelling sites in the elementary cell. The creation of the spin-down quasiparticle at these sites, (0, 0), (1, 0), (4, 1), (5, 1), induces the formation at the ladder leg of an uncompensated spin, the direction of which is parallel to the direction of the nearest spin in the domain. For the sake of simplicity we will concentrate in this paper on the propagation of the spin-up quasiparticle. Such a simplification is possible because despite the breakdown of the time-reversal symmetry by the underlying spin structure, the energy of the spin-up and the

spin-down quasiparticles is degenerate. Later we will use this observation in the calculation. Now we find the second diagonal term in the Hamiltonian describing the propagation of the spin-up polaron. The on-site energy of the spin-up hole-like quasiparticle is lower for some sites by $J/2$ than for sites to which the contribution (6) refers because the spin of the bond-fermion which is formed after a hole has been created at a bond initially occupied by a singlet is in this case antiparallel to the nearest spin in one of domains,

$$\delta_2 H_{\mathrm{eff}} = \tfrac{3}{2} J \sum_{m,n} \left[h^{\dagger}_{\binom{m,n}{0,0}\uparrow} h_{\binom{m,n}{0,0}\uparrow} + h^{\dagger}_{\binom{m,n}{1,0}\uparrow} h_{\binom{m,n}{1,0}\uparrow} + h^{\dagger}_{\binom{m,n}{4,1}\uparrow} h_{\binom{m,n}{4,1}\uparrow} + h^{\dagger}_{\binom{m,n}{5,1}\uparrow} h_{\binom{m,n}{5,1}\uparrow} \right]. \tag{7}$$

Let us concentrate now on the on-site energy of quasiparticles created at sites belonging to domains. By definition, a spin-up hole-like spin polaron can be created exclusively at sites which have been initially occupied by a spin-down fermion. An obvious contribution to the on-site energy of a hole-like quasiparticle energy in domains is ε_1, the minimum value of the matrix element (4) obtained under the constraint $\langle \Psi_i | \Psi_i \rangle = 1$. During the construction of spin polarons we have considered only hopping between NN sites, which is governed by the hopping with the highest integral t. We have also neglected some 'high-order' processes related to path crossing or to the action of the XY term in the Heisenberg model. In the analysis which we start now, we will discuss in the framework of the lowest-order perturbation theory the contribution of some neglected processes to the effective Hamiltonian H_{eff}. States depicted by figures 4(b) and (c) are string states of length 1 and are components of the spin polaron wavefunction $|\Psi_i\rangle$ at the site i. A single vertical or horizontal hop of the hole created in the AF background at the site i gives rise to the states depicted by figures 4(b) and (c) respectively. The hopping term to next-nearest neighbours (NNN) couples states represented by figures 4(b) and (c), which brings about a contribution to the matrix element $\langle \Psi_i | H_1 | \Psi_i \rangle$, where $H_1 = H - H_0$. This contribution is

$$\gamma_1 = 4t' \alpha_1^2. \tag{8}$$

We recognize in (8) a product of amplitudes with which string states of length 1 appear in the definition (2) of the spin polaron state. The factor 4 which appears in (8) is related to the fact that hopping which couples states (b) and (c) may occur in both directions and that analogous coupling takes place between the state depicted by figure 4(c) and the state depicted by figure 4(d). The state depicted by figure 4(d) has been obtained by a single downward hop of a hole created in the AF domain at the site i. The contribution

$$\gamma_2 = 2t'' \alpha_1^2 \tag{9}$$

to $\langle \Psi_i | H_1 | \Psi_i \rangle$ originates in a similar way with the coupling between states depicted in figures 4(c) and (d). That coupling is mediated by the hopping term to third-nearest-neighbour (TNN) sites. Matrix elements between longer string states which are components of the same spin polaron wavefunction may also contribute to the renormalization of the spin polaron on-site energy. To be more specific, the coupling between states as depicted by figures 4(e) and (f) and between their reflections in the horizontal line running through the site i gives rise to the correction

$$\gamma_3 = 2t' \left[2\alpha_2^2 + (z-1) \sum_{\mu=3} (z-2)^{\mu-3} \alpha_\mu^2 \right] \tag{10}$$

to $\langle \Psi_i | H_1 | \Psi_i \rangle$, while the coupling between the state depicted by figure 4(g) and its reflection in the horizontal line running through the site i together with some similar processes in which longer strings are involved brings about the correction

$$\gamma_4 = 2t'' \left[\alpha_2^2 + (z-1) \sum_{\mu=3} (z-2)^{\mu-3} \alpha_\mu^2 \right]. \tag{11}$$

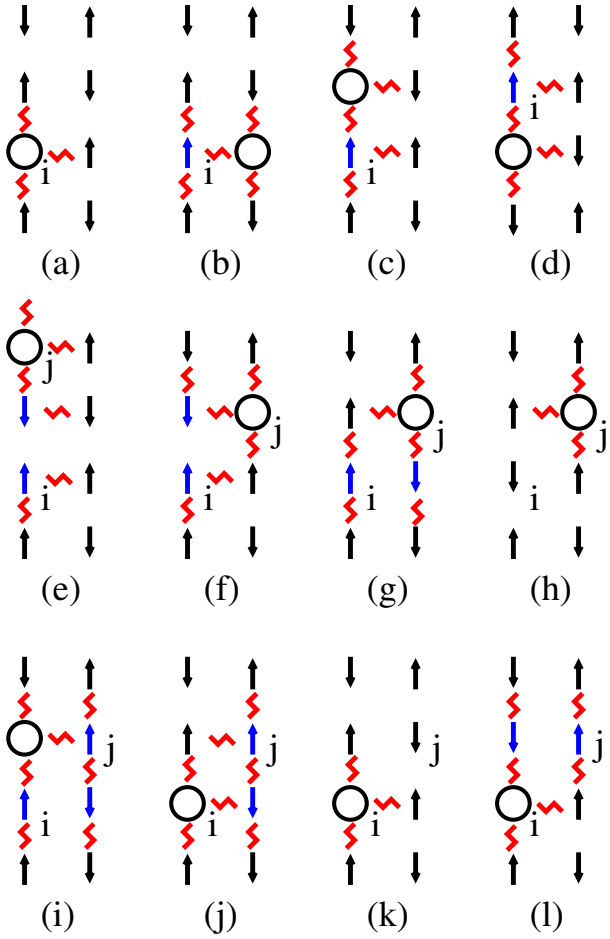

Figure 4. Illustration of processes contributing to some terms in the effective Hamiltonian. These terms define the on-site energy and the quasiparticle hopping between sites which belong to AF domains.

The states represented by figures 4(e)–(g) have been obtained by means of three different sequences of hole moves. The hole has been initially created at the site i. The sequences consist of two hops which are hops upwards–upwards, upwards–left and left–upwards, respectively. Longer strings pinned to the site i may be coupled in a very similar way, which also gives rise to a change of the on-site energy. This change has actually already been incorporated into parameters γ_3 and γ_4. Finally, by collecting all terms we may infer that in the effective Hamiltonian $H_{\rm eff}$ there appears the following term referring to the on-site energy of spin polarons:

$$\delta_3 H_{\rm eff} = (\varepsilon_1 + \gamma_1 + \gamma_2 + \gamma_3 + \gamma_4 + J/4) \times \sum_{m,n} \Big[h^{\dagger}_{\binom{m,n}{2,1}\uparrow} h_{\binom{m,n}{2,1}\uparrow} + h^{\dagger}_{\binom{m,n}{3,0}\uparrow} h_{\binom{m,n}{3,0}\uparrow} + h^{\dagger}_{\binom{m,n}{6,0}\uparrow} h_{\binom{m,n}{6,0}\uparrow} + h^{\dagger}_{\binom{m,n}{7,1}\uparrow} h_{\binom{m,n}{7,1}\uparrow} \Big]. \tag{12}$$

The additional term $J/4$ in the prefactor is related to the fact that the contribution from the contact interaction $-Jn_i n_j/4$ between a site i in a domain and a site j in a DW is higher by $J/4$, when a hole is created in the domain at the site i. This interaction was neglected when we were calculating the eigenenergy ε_1 of the spin polaron and needs to be taken into account now. (12) is the last on-site term in the effective Hamiltonian.

The NN hopping integral for the quasiparticle, the propagation of which we describe in this paper, is the same as the bare hopping integral provided that the sites between which the quasiparticle moves belong to the same initially ordered bond inside a DW [34]. Thus, the term which describes the quasiparticle hopping between NN sites, on which singlets have been formed in the underlying spin background, takes the following form:

$$\delta_4 H_{\mathrm{eff}} = -t \sum_{m,n} \Big\{ \big[h^{\dagger}_{\binom{m,n}{0,1}\uparrow} h_{\binom{m,n}{0,0}\uparrow} + h^{\dagger}_{\binom{m,n}{1,1}\uparrow} h_{\binom{m,n}{1,0}\uparrow} + h^{\dagger}_{\binom{m,n}{4,1}\uparrow} h_{\binom{m,n}{4,0}\uparrow} + h^{\dagger}_{\binom{m,n}{5,1}\uparrow} h_{\binom{m,n}{5,0}\uparrow} \big] + \mathrm{H.c.} \Big\}. \tag{13}$$

The NN hopping integral for a pair of sites which belong to different singlets in the underlying insulating state is $t/2$ instead of $-t$. The change of sign and the reduction of absolute value may be deduced from the form of the first term on the right-hand side of equation (36). Therefore, we may write the following expression for the contribution to the effective Hamiltonian describing quasiparticle hopping between NN sites belonging to different bonds on which singlets has been formed in the underlying spin background:

$$\delta_5 H_{\mathrm{eff}} = \frac{t}{2} \sum_{m,n} \Big\{ \big[h^{\dagger}_{\binom{m,n}{1,0}\uparrow} h_{\binom{m,n}{0,0}\uparrow} + h^{\dagger}_{\binom{m,n-1}{0,1}\uparrow} h_{\binom{m,n}{0,0}\uparrow} + h^{\dagger}_{\binom{m,n}{1,1}\uparrow} h_{\binom{m,n}{0,1}\uparrow} + h^{\dagger}_{\binom{m,n-1}{1,1}\uparrow} h_{\binom{m,n}{1,0}\uparrow} + h^{\dagger}_{\binom{m,n}{5,0}\uparrow} h_{\binom{m,n}{4,0}\uparrow} + h^{\dagger}_{\binom{m,n-1}{4,1}\uparrow} h_{\binom{m,n}{4,0}\uparrow} + h^{\dagger}_{\binom{m,n}{5,1}\uparrow} h_{\binom{m,n}{4,1}\uparrow} + h^{\dagger}_{\binom{m,n-1}{5,1}\uparrow} h_{\binom{m,n}{5,0}\uparrow} \big] + \mathrm{H.c.} \Big\}. \tag{14}$$

The value of the NN hopping integral, between a site which belongs to a domain and a site which belongs a DW, can be inferred from the first part of the right-hand side in equation (38). The prefactor in a term which represents that process contains the amplitude α_0 of zero length string states,

$$\delta_6 H_{\mathrm{eff}} = -\frac{t}{\sqrt{2}} \alpha_0 \sum_{m,n} \Big\{ \big[h^{\dagger}_{\binom{m,n-1}{7,1}\uparrow} h_{\binom{m,n}{0,1}\uparrow} + h^{\dagger}_{\binom{m,n}{2,1}\uparrow} h_{\binom{m,n}{1,1}\uparrow} + h^{\dagger}_{\binom{m,n}{3,0}\uparrow} h_{\binom{m,n}{4,0}\uparrow} + h^{\dagger}_{\binom{m,n}{6,0}\uparrow} h_{\binom{m,n}{5,0}\uparrow} \big] + \mathrm{H.c.} \Big\}. \tag{15}$$

Since the time-reversal symmetry and the translational symmetry are broken inside AF domains, the propagating quasiparticle cannot move between different sublattices and no term related to NN hopping inside domains is generated in the effective Hamiltonian H_{eff}. NNN quasiparticle hopping inside DWs and hopping between sites which belong to a DW and a domain is a first-order process that is mediated by the NNN hopping term in the bare Hamiltonian. The explicit forms of related contributions to H_{eff} may be deduced from formulae (36)–(38),

$$\delta_7 H_{\mathrm{eff}} = \frac{t'}{2} \sum_{m,n} \Big\{ \big[h^{\dagger}_{\binom{m,n}{1,1}\uparrow} h_{\binom{m,n}{0,0}\uparrow} + h^{\dagger}_{\binom{m,n-1}{1,1}\uparrow} h_{\binom{m,n}{0,0}\uparrow} + h^{\dagger}_{\binom{m,n}{1,0}\uparrow} h_{\binom{m,n}{0,1}\uparrow} + h^{\dagger}_{\binom{m,n-1}{0,1}\uparrow} h_{\binom{m,n}{1,0}\uparrow} + h^{\dagger}_{\binom{m,n}{5,1}\uparrow} h_{\binom{m,n}{4,0}\uparrow} + h^{\dagger}_{\binom{m,n-1}{5,1}\uparrow} h_{\binom{m,n}{4,0}\uparrow} + h^{\dagger}_{\binom{m,n}{5,0}\uparrow} h_{\binom{m,n}{4,1}\uparrow} + h^{\dagger}_{\binom{m,n-1}{4,1}\uparrow} h_{\binom{m,n}{5,0}\uparrow} \big] + \mathrm{H.c.} \Big\}, \tag{16}$$

$$\delta_8 H_{\mathrm{eff}} = -\frac{t'}{\sqrt{2}} \alpha_0 \sum_{m,n} \Big\{ \big[h^{\dagger}_{\binom{m-1,n}{7,1}\uparrow} h_{\binom{m,n}{0,0}\uparrow} + h^{\dagger}_{\binom{m-1,n-1}{7,1}\uparrow} h_{\binom{m,n}{0,0}\uparrow} + h^{\dagger}_{\binom{m,n}{2,1}\uparrow} h_{\binom{m,n}{0,0}\uparrow}$$

$$+ h^{\dagger}_{\binom{m,n-1}{2,1}\uparrow} h_{\binom{m,n}{0,0}\uparrow} + h^{\dagger}_{\binom{m,n}{3,0}\uparrow} h_{\binom{m,n}{4,1}\uparrow} + h^{\dagger}_{\binom{m,n+1}{3,0}\uparrow} h_{\binom{m,n}{4,1}\uparrow} + h^{\dagger}_{\binom{m,n}{6,0}\uparrow} h_{\binom{m,n}{5,1}\uparrow}$$
$$+ h^{\dagger}_{\binom{m,n+1}{6,0}\uparrow} h_{\binom{m,n}{5,1}\uparrow}\Big] + \text{H.c.}\Big\}. \tag{17}$$

The task of finding the formula for the term describing NNN hopping inside AF domains is slightly more tedious. For example the coupling by the XY term in the Heisenberg model between string states depicted by figures 4(f) and (h) gives rise to hopping terms in H_{eff} which shift a spin polaron from the site i to the site j and vice versa. We analyse now the XY term, because it has been neglected during the first stage of the analysis, when quasi-confined spin polaron states have been constructed. Since the string state depicted by figure 4(f) is a component of the wavefunction $|\Psi_i\rangle$ for the spin polaron created at the site i and the string state depicted by figure 4(h) is evidently a component of the wavefunction for the spin polaron created at the site j, the coupling between these components gives rise to the coupling between spin polaron states $|\Psi_i\rangle$ and $|\Psi_j\rangle$. This brings about a contribution to the matrix element $\langle\Psi_j|H|\Psi_i\rangle$ and to the hopping term in the effective Hamiltonian H_{eff}. Also the coupling between the states depicted by figures 4(g) and (h) contributes to the hopping term between the sites i and j in H_{eff}. This coupling is mediated by the XY term. We have just discussed the action of the XY term which by removing two defects in the AF structure transforms string states of length 2, tails of which are pinned to the site i, into the state representing a hole created at the site j in the AF ordered domain. By a string tail we mean its end opposite the end at which sits a hole. The XY term may transform in an analogous way a state representing a hole created in the domain at the site i into a string state of length 2 pinned at the tail to the site j. This additional coupling between components of the spin polaron states at the sites i and j doubles the value of the hopping integral between these sites in the effective Hamiltonian. Thus, after a little thought we may deduce that an appropriate contribution to the integral for the NNN hopping of quasiparticles inside domains is

$$\tau_1 = 2J \sum_{\mu=2} (z-2)^{\mu-2} \alpha_\mu \alpha_{\mu-2}. \tag{18}$$

The first term in the sum presented above refers to coupling between strings of length 0 and 2. We have just outlined its origin in detail. Other terms appear in the sum (18) because longer strings, which are created when a hole moves further from the site j in figures 4(f)–(h), are also coupled by the XY term in the Heisenberg model. The hop left of the hole depicted by figure 4(g) gives rise to the string state of length 3, figure 4(i), which is pinned to the site j. Since we have neglected the possibility of path crossing when we were constructing the quasi-confined spin polaron states, some corrections need to be made now. For example, we have not considered before that by applying the NN hopping term to the state depicted by figure 4(i) we may create the state depicted by figure 4(j). Since the latter state is a string-like component of the spin polaron at the site j obtained by hopping downwards and left of a hole created at that site, we deduce that the process described above generates a contribution to the prefactor of the NNN hopping term in the effective Hamiltonian,

$$\tau_2 = 2t\alpha_3\alpha_2. \tag{19}$$

The factor 2 originates from the fact that the motion of a hole around a plaquette in the square lattice may take place clockwise and anticlockwise. We also recognize α_3 and α_2 as amplitudes of strings, which have the length 3 and 2, respectively. Exactly such strings which are components of the spin polaron states at the sites i and j in figures 4(i), (j) are coupled by the NN hopping term in the initial Hamiltonian. The NNN term in the initial Hamiltonian generates coupling between states representing 'bare' holes created in the AF background of domains. Since these states are also string components with the length 0 of some spin polaron

wavefunctions, coupling between the latter is also generated. Examples of such coupled string states are figures 4(h) and (k). The contribution to the NNN hopping integral in $H_{\rm eff}$ is

$$\tau_3 = t'\alpha_0^2. \tag{20}$$

The NNN term in the bare Hamiltonian also couples states depicted by figures 4(f) and (l) which are string-like components with length 2 of spin polaron states at the sites i and j, respectively. The coupling amplitude is

$$\tau_4 = 2t'\alpha_2^2. \tag{21}$$

The appearance of the factor 2 is related to the fact that states which are created when holes move between the sites i and j in opposite directions around the plaquette, as in the case of the states depicted by figures 4(f) and (l), are also coupled by the bare NNN hopping. The state in figure 4(l) has been obtained by hopping left and downwards of a hole which has been initially created at the site j. By collecting all contributions, which we have discussed above, we see that the new term in $H_{\rm eff}$ is

$$\delta_9 H_{\rm eff} = (\tau_1+\tau_2+\tau_3+\tau_4)\times\sum_{m,n}\Big\{\big[h^{\dagger}_{\binom{m,n}{3,0}\uparrow}h_{\binom{m,n}{2,1}\uparrow}+h^{\dagger}_{\binom{m,n-1}{2,1}\uparrow}h_{\binom{m,n}{3,0}\uparrow}+h^{\dagger}_{\binom{m,n}{7,1}\uparrow}h_{\binom{m,n}{6,0}\uparrow} + h^{\dagger}_{\binom{m,n-1}{7,1}\uparrow}h_{\binom{m,n}{6,0}\uparrow}\big]+\text{H.c.}\Big\}. \tag{22}$$

By means of a similar analysis as for the hopping between NNN sites we may find the TNN hopping term in the effective Hamiltonian. For the operator representing the quasiparticle hopping inside DWs we get

$$\begin{aligned}\delta_{10}H_{\rm eff} = \frac{t''}{2}\sum_{m,n}\Big\{&\big[h^{\dagger}_{\binom{m,n+1}{0,0}\uparrow}h_{\binom{m,n}{0,0}\uparrow}+h^{\dagger}_{\binom{m,n+1}{0,1}\uparrow}h_{\binom{m,n}{0,1}\uparrow}+h^{\dagger}_{\binom{m,n+1}{1,0}\uparrow}h_{\binom{m,n}{1,0}\uparrow}\\ &+h^{\dagger}_{\binom{m,n+1}{1,1}\uparrow}h_{\binom{m,n}{1,1}\uparrow}+h^{\dagger}_{\binom{m,n+1}{4,0}\uparrow}h_{\binom{m,n}{4,0}\uparrow}+h^{\dagger}_{\binom{m,n+1}{4,1}\uparrow}h_{\binom{m,n}{4,1}\uparrow}+h^{\dagger}_{\binom{m,n+1}{5,0}\uparrow}h_{\binom{m,n}{5,0}\uparrow}\\ &+h^{\dagger}_{\binom{m,n+1}{5,1}\uparrow}h_{\binom{m,n}{5,1}\uparrow}\big]+\text{H.c.}\Big\}.\end{aligned} \tag{23}$$

The TNN hopping of the quasiparticle between domains and DWs is governed by the following term:

$$\begin{aligned}\delta_{11}H_{\rm eff} = -\frac{t''}{\sqrt{2}}\alpha_0\sum_{m,n}\Big\{&\big[h^{\dagger}_{\binom{m-1,n}{0,0}\uparrow}h_{\binom{m,n}{0,0}\uparrow}+h^{\dagger}_{\binom{m,n}{2,1}\uparrow}h_{\binom{m,n}{0,1}\uparrow}+h^{\dagger}_{\binom{m,n}{3,0}\uparrow}h_{\binom{m,n}{1,0}\uparrow}\\ &+h^{\dagger}_{\binom{m-1,n}{7,1}\uparrow}h_{\binom{m,n}{1,1}\uparrow}+h^{\dagger}_{\binom{m,n}{6,0}\uparrow}h_{\binom{m,n}{4,0}\uparrow}+h^{\dagger}_{\binom{m,n}{2,1}\uparrow}h_{\binom{m,n}{4,1}\uparrow}+h^{\dagger}_{\binom{m,n}{3,0}\uparrow}h_{\binom{m,n}{5,0}\uparrow}\\ &+h^{\dagger}_{\binom{m,n}{7,1}\uparrow}h_{\binom{m,n}{5,1}\uparrow}\big]+\text{H.c.}\Big\}.\end{aligned} \tag{24}$$

To the TNN hopping term between sites in domains contribute: (a) the mechanism which is based on the shortening of strings by the action of the XY term, (b) the coupling of strings with length 0 by the TNN hopping term in the initial Hamiltonian and (c) the exchange between the head and the tail of a straight string with length 2. The last process is mediated by the TNN hopping term in the initial Hamiltonian (1).

The contributions to the hopping integral in these three cases are

$$\tau_5 = 2J\sum_{\mu=2}(z-2)^{\mu-2}\alpha_\mu\alpha_{\mu-2}, \tag{25}$$

$$\tau_6 = t''\alpha_0^2, \tag{26}$$

$$\tau_7 = t''\alpha_2^2. \tag{27}$$

Since the origin of these couplings is the same as for the NNN hopping term in $H_{\rm eff}$ we do not discuss them in detail. Thus, the TNN hopping operator, which is the last contribution to $H_{\rm eff}$ discussed by us at the approximation level, that we have applied, takes the form

$$\delta_{12}H_{\rm eff} = (\tau_5+\tau_6+\tau_7)\sum_{m,n}\Big\{\big[h^{\dagger}_{\binom{m,n+1}{2,1}\uparrow}h_{\binom{m,n}{2,1}\uparrow} + h^{\dagger}_{\binom{m,n+1}{3,0}\uparrow}h_{\binom{m,n}{3,0}\uparrow} + h^{\dagger}_{\binom{m,n+1}{6,0}\uparrow}h_{\binom{m,n}{6,0}\uparrow} + h^{\dagger}_{\binom{m,n+1}{7,1}\uparrow}h_{\binom{m,n}{7,1}\uparrow}\big] + \text{H.c.}\Big\}. \tag{28}$$

Figure 6 depicts the electronic structure which we have obtained by solving the Hamiltonian $H_{\rm eff}$. It represents the energy dispersion $E(\mathbf{p})$ of all bands along the line $(0,0)$–$(\pi,0)$–(π,π)–$(0,0)$ and the line obtained by performing the rotation by $\pi/2$ around the point $(0,0)$. Such a combination of dispersion curves is justified by conditions in which experiments are performed, because it seems that stripes in some regions of the sample may run vertically, while in other regions they may run horizontally. The reason for this mixing can be, for example, sample twinning. Nondispersing parts of bands are related to some obstacles for hole propagation in the directions perpendicular to stripes. That kind of motion seems to be at least partially blocked, which is clear because $H_{\rm eff}$ by definition cannot mediate quasiparticle motion occurring exclusively in the direction perpendicular to stripes. It seems that the lack of the energy dispersion in some directions accounts for straight patches of the spectral weight which appear in the density maps obtained by means of ARPES measurements [42]. The frame of reference applied to draw these maps is the same as we have used to obtain figure 6 (momentum–energy), while the second derivative of ARPES spectra plays the role of a density-like parameter which marks regions with high spectral weight [28]. We shall make a more detailed comparison with ARPES spectra after we calculate the spectral weight by means of our approach, which is a combination of bond and string formalisms.

3. Single-particle spectral function in the stripe phase with coexisting bond and AF orders

ARPES probes the one-particle spectral function $A^{-}(\mathbf{k},\omega)$. In our analysis of ARPES spectra in the stripe phase of cuprates we neglect the influence of temperature. We also assume that the description of the photoelectric effect in terms of Fermi's golden rule is sufficient and, furthermore, we omit in the calculation electromagnetic dipole matrix elements between the wavefunction of a photoelectron and the wavefunctions of electrons in initial states. We apply the single-particle approximation in the calculation of the spectral function $A^{-}(\mathbf{k},\omega)$, which is natural, because the Hamiltonian $H_{\rm eff}$ by definition does not contain the interaction terms. Since electrons are emitted during the photoelectric process, information is gathered at $T=0$ only about the one-electron removal part of the spectral function, which can be written as

$$A^{-}(\mathbf{k},\omega) = \sum_{m}|\langle\Psi_m^{N-1}|c_{\mathbf{k}\downarrow}|\Psi_0^{N}\rangle|^2\delta(\omega+E_m^{N-1}-E_0^{N}). \tag{29}$$

$|\Psi_0^N\rangle$ and $|\Psi_m^N\rangle$ denote the ground state and exited states of a system with N electrons, respectively. Due to the formation of the stripe structure, the shape of which is determined by the underlying spin background depicted by figure 1, the first Brillouin zone (1BZ) gets reduced by a factor of 8 in the horizontal direction and by a factor of 2 in the vertical direction. The Hamiltonian $H_{\rm eff}$ may be written in diagonal form in terms of operators $h^{\dagger}_{\mathbf{k},\uparrow,\alpha}$, and their Hermitian conjugates, which are determined by the form of Hamiltonian eigenstates,

$$h^{\dagger}_{\mathbf{k_R},\uparrow,\alpha} = \frac{1}{\sqrt{DW}}\sum_{n,l}\mathrm{e}^{\mathrm{i}\mathbf{k}_R(nd,lw)}\sum_{i,j}F_{\mathbf{k}_R,(i,j),\uparrow,\alpha}h^{\dagger}_{\binom{n,l}{i,j}\uparrow} \tag{30}$$

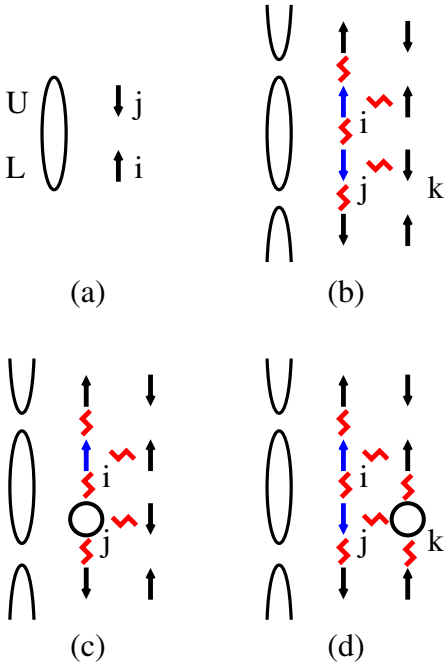

Figure 5. Graphical representation of states involved in the generation of quantum fluctuations in $|\Omega\rangle$. Contributions from these fluctuations determine to a large extent the shape of the spectral function.

where $\mathbf{k}_R$ belongs to the reduced 1BZ, α labels the band number, $d = 8$ is the length of the elementary supercell, $w = 2$ is the width of the elementary supercell and $Dd \times Ww$ is the system size. Thus, within the single-particle approach, the one-electron removal part of the spectral function is

$$A^-(\mathbf{k},\omega) = \sum_{\alpha} \delta(\omega + \varepsilon_{\mathbf{k},\alpha}) | \sum_{n,l} \sum_{i,j} \sum_{i',j'} F^*_{\mathbf{k},\mathrm{mod}\mathbf{K}_R,(i,j);\uparrow,\alpha} \mathrm{e}^{\mathrm{i}\mathbf{k}(nd,lw)} \mathrm{e}^{-\mathrm{i}\mathbf{k}(i',j')} \times \langle\Omega| h^{\dagger}_{\binom{n,l}{i,j}\uparrow} c_{\binom{0,0}{i',j'}\downarrow} |\Omega\rangle|^2, \tag{31}$$

where $\mathbf{k}\mathrm{mod}\mathbf{K}_R$ denotes the vector $\mathbf{k}$ reduced to the 1BZ of the superlattice, the elementary cell of which is depicted by figure 1, and $\varepsilon_{\mathbf{k},\alpha}$ is the energy of the αth band in figure 6. In order to evaluate (31) we need to find matrix elements,

$$M_{\binom{n,l}{i,j}\binom{0,0}{i',j'}} = \langle\Omega| h^{\dagger}_{\binom{n,l}{i,j}\uparrow} c_{\binom{0,0}{i',j'}\downarrow} |\Omega\rangle. \tag{32}$$

A scheme showing how to do this in the framework of the spin polaron (string) approach was developed before [43]. For example, the removal of the spin-down electron at the site (2, 1) in the elementary cell of the underlying spin background depicted by figure 1 gives rise to a state which is a component of the wavefunction for the polaron created at this site. Thus the matrix element (32) for $(i', j') = (i, j) = (2, 1)$ and $(n, l) = 0$ is α_0.

Quantum spin fluctuations which are generated in the underlying spin background schematically depicted by figure 1 cannot be neglected when we evaluate the spectral function. Within the first-order perturbation theory the admixture $\delta|\phi\rangle$ of quantum fluctuations to the ground state $|\phi_0\rangle$ of H_0 brought about by the perturbation H_1 is

$$\delta|\phi\rangle = -\sum_n \frac{\langle\psi_n|H_1|\phi_0\rangle}{E_n - E_0} |\psi_n\rangle, \tag{33}$$

where $|\psi_n\rangle$ are excited eigenstates of H_0 with energies E_n and E_0 is the ground-state energy. The action of the exchange interaction between sites depicted by figure 5(a), $L(U)$ belonging

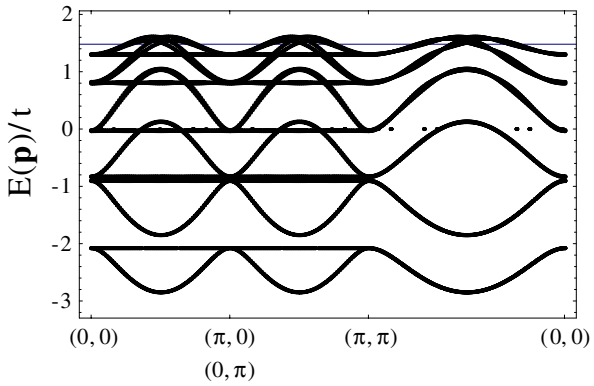

Figure 6. Band structure in the stripe phase, obtained within the scenario of coexisting bond and AF orders.

to a DW and $i\,(j)$ belonging to an AF domain, may transform the singlet on sites L and U into a triplet. Within our approach we treat this part of the exchange interaction as the perturbation. The transformed state is an excited eigenstate of H_0 with the energy J and also a quantum fluctuation that, according to the formula (33), contributes to the underlying vacuum state $|\Omega\rangle$, about which we assume that it is an eigenstate of the Hamiltonian (1). In figure 1 which is the graphical representation of a lowest-order approximation to $|\Omega\rangle$ quantum corrections have not been taken into account. The electron annihilation operator c that acts on a site belonging to a bond, on which a triplet excitation has been formed, transforms it into the state representing the hole-like quasiparticle h created at that site. This process gives rise to an addendum to the matrix element (32). For example, the value of this addendum is $-1/(2\sqrt{2})$ for the matrix element (32) labelled by the indices $(i', j') = (i, j) = (n, l) = (0, 0)$. The XY part of the exchange interaction, which we treat as a perturbation, creates in $|\Omega\rangle$ an excitation that takes the form of two NN spins turned upside down, figure 5(b), in comparison to the underlying spin structure, figure 1. According to the recipe (33) this excitation contributes a correction to the underlying vacuum state $|\Omega\rangle$. If the annihilation operator c removes the spin-down fermion at the site j in figure 5(b), the configuration depicted by figure 5(c) will be created, which is a string state, a component of the wavefunction $|\psi_i\rangle$ for the spin polaron at the site i. Since this spin polaron state is by definition created by the fermionic operator $h_i^\dagger$ a contribution $-\alpha_1/4$ to some diagonal matrix elements of the form (32) is generated. Now, we discuss the last category of processes which create new terms in the sum that appears in (31). The electron removal from the site k, figure 4(b), gives rise to a string state of length 2, figure 4(d), which is a component of the wavefunction for the spin polaron at the site i. Since the spin polaron state is created by the operator $h_i^\dagger$, a nonvanishing matrix element in M defined by (32) is generated. Its value is $-\alpha_2/4$, which gets multiplied by a factor of 2, because there are two strings of length 2, connecting sites i and k. By collecting all contributions to the sum which appears in (31) the one-electron removal part of the spectral function $A^-(\mathbf{k}, \omega)$ can be evaluated. We will apply in the numerical evaluation some Lorentzian broadening of the Dirac delta function, which is justified because experimental measurements, with which we are going to compare our results, have finite resolution and also an averaging procedure is often applied to present experimental data.

The removal of a spin-down electron from a site which belongs to a ladder-like DW in the state depicted by figure 1 gives rise to the hole-like quasiparticle h at this site. Since this removal may be induced by the electron annihilation operator c in (32), a nonvanishing diagonal matrix element $-1/\sqrt{2}$ is generated.

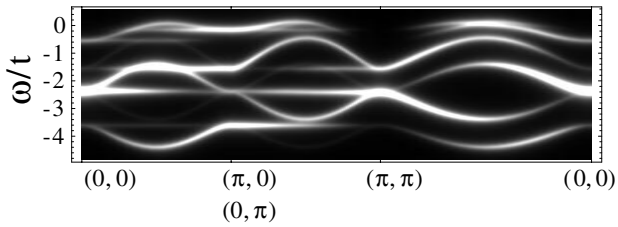

Figure 7. Spectral weight intensity $A^{-}(\mathbf{k}, \omega)$ along some directions at the doping level 15%. Lorentzian broadening with the width $0.1t$ has been applied.

In a similar way as has been shown above, all nonvanishing matrix elements (32) may be found within the applied approach.

4. Numerical evaluation of the spectral weight, comparison with results of ARPES experiments and concluding remarks

It seems that the most complete set of data to compare with our theoretical analysis provides ARPES measurements of the LSCO and Nd-LSCO systems made for the doping level $x = 0.15$ [13, 14, 28, 42]. We will present our results in a way similar to the presentation method, which was used in experimental papers reporting these measurements. The NN hopping parameter t defines a unit in which energy is measured. We choose $J/t = 0.4$, $t'/t = -0.1$, $t''/t = 0.05$. That choice is based on several previous theoretical analyses by means of which model parameters have been determined by making comparison with ARPES spectra of different cuprate compounds [44–51]. Similar values of parameters have also been applied in a recent theoretical analysis of ARPES spectra in the 2D tJM [32]. That analysis is based on the exact diagonalization of the 5×4 cluster. The same parameters have been used in a separate calculation presented in that paper and performed by means of the bond operator formalism applied to the underlying spin structure with the columnar bond order. This coincidence helps to make comparison between the results of the calculation presented in our paper and the results of the earlier analysis. Furthermore, previous discussions of ARPES spectra from LSCO systems indicate that the ratios $|t'/t|$ and $|t''/t|$ are lower for these systems than for other members of cuprate family [51], which agrees with our choice.

The position of the Fermi energy in the band structure at the doping level 15% has been determined in our calculation by counting the number of hole-like states. It has been marked as a narrow straight line in figure 6. Figure 7 depicts the intensity of the one-electron removal spectrum function presented in the frame of reference momentum–energy. Contributions from vertical and horizontal stripes have been summed in order to account for the presumed coexistence of these structures in different parts of the sample. In some agreement with the experimental result obtained at the doping level 15% [28] we notice in the calculated spectrum a strongly dispersing band between points $(0, 0)$ and $(\pi, 0)/(0, \pi)$ which approaches the Fermi level, $\omega = 0$, near the zone boundary, where it joins a flat patch formed by the region of high spectral intensity. After passing the antinodal region as a straight narrow strip, the band-like region of high intensity disappears somewhere between $(\pi, 0)/(0, \pi)$ and (π, π) points. In the calculated spectrum we also notice two cusps near $\mathbf{k} = (\pi/2, 0)$ and $\mathbf{k} = (\pi, \pi/2)$. Those cusps are absent in the experimental spectrum. This discrepancy may be attributed to the fact that to the just discussed high-intensity patch which looks like a single band in the plot there actually contribute two of many bands which may be seen in figure 6.

Notwithstanding some more discrepancies, we will see that our approach gives rise to results that are in overall agreement with experimental data, which is not true if the propagation of a hole in a homogeneous AF background or in a pure bond-ordered background is considered. For example, the band which appears in the results of the calculation based on the scenario of the columnar bond order [32] also has strong dispersion but does not flatten in the antinodal region. Despite the fact that neither the spectral weight of a quasiparticle propagating in the bond-ordered spin background nor the spectral weight of the quasiparticle propagating in the AF background [52] resembles ARPES spectra from doped LSCO and doped Nd-LSCO in the stripe phase, the spectral properties of our model in which these two phases coexist are in qualitative agreement with experimental data. This agreement may be attributed to the fact that the band structure of the model for nanoscale phase separation which we discuss here has some features which are present in band structures of both pure homogeneous phases. We will justify this statement during the further analysis of the spectrum. For example, in our results we actually see a remnant of a strip formed by a high-intensity region which takes the shape of a strongly dispersing band along the line between points $(0, 0)$ and $(\pi, 0)/(0, \pi)$ and resembles the band that is formed in the columnar bond-ordered phase. This band-like structure actually does not flatten and reaches a maximum near the points $(0, \pi/2)/(\pi/2, 0)$. It is likely that the presence of this maximum in our calculation may be attributed to the brute force method of sewing the bond-ordered parts of the system with the parts which are antiferromagnetically ordered. The lack of the straight high-intensity patch at the antinodal region in results of the theory based on the scenario of the columnar bond-ordered phase gives rise to a conclusion that the spectral function calculated within this picture does not satisfactorily agree with measured ARPES spectra and suggests that it is necessary to take into account the long-range AF correlations in order to formulate a theory which accounts for the spectral properties of the cuprates in the stripe phase.

In the region between the zone centre and antinodal points $(\pi, 0)/(0, \pi)$ the agreement has been also observed between the experimental data and the results of a calculation based on the dynamical mean field theory (DMFT) applied to the Hubbard model [18].

Along the line connecting the points $(0, 0)$ and (π, π) both in ARPES spectra and in our results we see a band in the vicinity of the Fermi surface. This band has a maximum at the points $(\pi/2, \pi/2)$, bends downwards, and disappears near the zone corner. A similar feature may be observed in the results of an exact diagonalization performed for the t–t'–t''–J model and in the results of the calculation performed within the scenario of the bond-ordered columnar phase [32]. The DMFT of the stripe phase in the Hubbard model at the doping level 15% gives rise to a slightly different result, namely it seems that the band crosses the Fermi level near the point $(\pi/2, \pi/2)$.

The intensity map of the one-electron removal spectral function $A^{-}(\mathbf{k}, \omega)$ at the Fermi energy obtained in the framework of our scenario which assumes the coexistence of bond and AF orders is depicted by figure 8. Figure 8(a) refers to results of the calculation in which we have assumed that bond order is formed on legs in ladder-like DWs. That figure shows some agreement with ARPES data from LSCO and Nd-LSCO [14] obtained for the doping level 15%. We see well developed spectral weight in the antinodal regions. These regions are bridged by high-intensity continuous almost straight high-intensity patches. It seems that the agreement between the experimental results and the results of our theory based on the mixture of the bond formalism and the spin polaron approach is slightly better in this respect than the agreement with results of the previous calculations based on the CPT applied to microscopic models which are the $t\,J$M and the Hubbard model [21, 26].

Figure 8(b) depicts the spectral weight at the Fermi energy obtained in a separate calculation for the underlying spin background with bond order on rungs. We know from

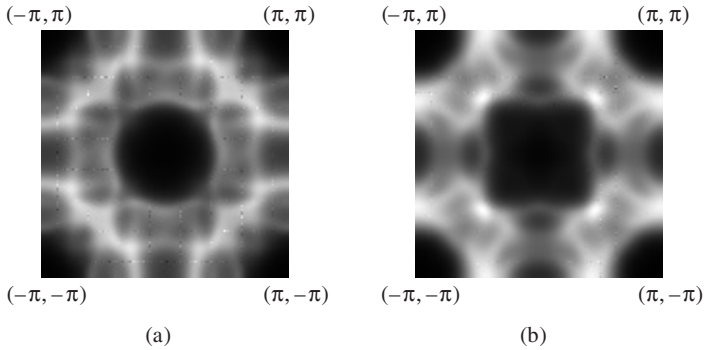

Figure 8. Intensity maps of the spectral weight $A^{-}(\mathbf{k}, \omega)$ at E_{F} obtained for stipe systems with bond order on legs (a) and with bond order on rungs (b).

the results of a previous paper [34] that such a structure is less stable and do not expect much similarity with experimental results. Such a lack of similarity may be seen, indeed. For example, the high-intensity patches do not form a shape resembling the Fermi surface obtained by means of calculations based on the local density approach. Such a shape may be observed both in experimental spectra and in figure 8(a). In figure 8 apart from patches of high spectral density along curves forming the Fermi surface which is observed in experiments we notice additional regular structures formed by regions of enhanced intensity. It seems that the origin of those additional structures may be attributed to simplicity of our approach within which fluctuations of the underlying spin structure depicted in figure 1 and shape fluctuations of stripes are neglected to a great extent. It is natural to expect that such fluctuations smear out the contribution to the spectral function from excitations which may be classified as incoherent background and only the dominating quasiparticle contributions, which may be seen as very bright patches in figure 8, are preserved in the spectra of a real system.

Calculations based on the phenomenological approach to disordered charge stripes and antiphase spin domains give rise to a pattern formed by regions of high spectral intensity in the 1BZ which strongly resembles ARPES spectra [29, 25]. Unfortunately no microscopic justification has been provided for phenomenological one-body Hamiltonians which have been applied to derive the spectral density by means of calculations that rely on this scenario. Our calculation is based on the microscopic t–t'–t''–J model. On the other hand, it seems that disorder may give rise to spreading of spectral weight over the whole antinodal region. Such a spreading is not observed in the results of our calculation. In a previous paper we have demonstrated that the magnetic structure of the stripe which we have considered here is likely to have lowest energy at and above the doping level 12.5%, if the distance between axes of nearest stripes is 4 lattice spacings, as it has been suggested by experiments [34]. Bond order parallel to stripe axes and long-range AF order coexist in this magnetic structure.

It has been also suggested that the shape of the Fermi surface seen in ARPES spectra from Nd-LSCO and LSCO at the doping level in the range 12.5%–15% may be also explained in the framework of more conventional band calculations which neglect the formation of nanoscale inhomogeneities [53]. In our opinion, it is hard to reconcile such a way of thinking with the evidence for stripes forming in these systems.

A natural additional question which can be raised is whether the long-range Coulomb interaction will destabilize stripes. On the contrary, it seems that such interaction may even favour smectic order [54], especially when holes form bound pairs. In addition, the formation of wide stripes which are considered by us as bond-centred stripes does not mean that the

distance between nearest charges in stripes is much smaller than the average distance between all nearest charges. Thus the increase of the Coulomb energy induced by the nanoscale phase separation in the stripe phase is not necessary very high. On the other hand, a detailed analysis of the impact which the long-range Coulomb interaction between unbound charged holes may have on stripe formation is still missing. It is necessary to mention here that in this paper we analyse just the case of unbound charges and we do not discuss the issue of the long-range Coulomb forces. Nevertheless one can speculate that since the coherence length in cuprates is short the screening of the Coulomb repulsion should be substantial. Otherwise the applicability to cuprates of widely used models based on the Hubbard model would be questionable. The conclusion concerning screening is to some extent supported by the lack of clear evidence for the strong lattice response to local charge-stripe order [9–11, 55]. These remarks seem to suggest that in the simplest analysis of spectral properties in the bond-ordered stripe phase effects related to the long-range Coulomb interaction and lattice response can be neglected.

In conclusion, motivated by results of a previous calculation [34] indicating that, at the doping level $1/8$ and above, the stripe structure which consists of (a) hole-filled two-leg ladder-like DWs with the bond order formed on legs and (b) AF domains of width 2 lattice spacings and with the changing phase of the sublattice magnetization by π across each DW is stable, we have performed the calculation of the single-particle spectral density which is generated in such a system. Our analysis has been made in the framework of the t–t'–t''–J model with parameter values in the range suggested by comparison between band structure calculations and the Fermi surface of overdoped LSCO systems. The calculation which we have performed is a combination of the bond fermion method and the spin polaron approach. We observe pronounced spectral weight both in the antinodal and nodal regions. Very similar features may be seen in ARPES spectra from LSCO and Nd-LSCO at the filling level 15%, which is exactly the same as we have assumed in the calculation. This similarity is not trivial because different optional structures of bond order in DWs such as the bond order on rungs in the ladder-like DWs or the bond order which takes the shape of two layers in a brick-wall give rise to spectra at the Fermi level which have completely different forms. We consider the observed agreement between experiment and theory as an argument for the scenario of coexisting bond and long-range AF orders in the stripe phase of doped cuprates.

Acknowledgments

PW acknowledges useful discussions with P Fulde, R S Markiewicz, T T Nguyen and, A M Oleś.

Appendix

A singlet on two sites L and U is created in the empty lattice by the operator

$$s^{\dagger}_{LU} = \frac{\mathrm{i}}{\sqrt{2}}[\sigma^0\sigma^y]_{\alpha\beta}c^{\dagger}_{L\alpha}c^{\dagger}_{U\beta}. \tag{34}$$

σ^0 is the two-dimensional identity matrix and σ^a, $a = x, y, z$, are Pauli matrices. The summation over repeating Greek indices is assumed. Three operators which are components of the vector $\mathbf{t}^{\dagger}_{LU}$ create three triplet states on sites L and U,

$$\mathbf{t}^{\dagger}_{LU} = \frac{\mathrm{i}}{\sqrt{2}}[\sigma\sigma^y]_{\alpha\beta}c^{\dagger}_{L\alpha}c^{\dagger}_{U\beta}. \tag{35}$$

A formula which we often use is

$$-c^{\dagger}_{U'\sigma}c_{U\sigma}(s^{\dagger}_{LU}c^{\dagger}_{L'\gamma})|0\rangle = \left(\tfrac{1}{2}s^{\dagger}_{L'U'}c^{\dagger}_{L\gamma} + \tfrac{1}{2}\mathbf{t}^{\dagger}_{L'U'}\sigma_{\alpha\gamma}c^{\dagger}_{L\alpha}\right)|0\rangle. \tag{36}$$

The left-hand side of (36) together with the first term on the right-hand side represent the exchange of a singlet and a hole–fermion pair between two bonds. That exchange is mediated by the hopping term in the initial Hamiltonian. In our analysis we neglect the creation of triplets on bonds; however, this process also takes place during hole hopping. The creation of a triplet is represented by the second term on the right-hand side of (36). For calculation of the energy spectrum we also need formulae which represent the hopping of a hole from a single site i which belongs to an AF domain to a site which belongs to a bond occupied by a singlet and vice versa:

$$-c^{\dagger}_{i\sigma}c_{U\sigma}(s^{\dagger}_{LU})|\Omega\rangle = -\frac{\mathrm{i}}{\sqrt{2}}\sigma^{y}_{\alpha\beta}c^{\dagger}_{L\alpha}c^{\dagger}_{i\beta}|0\rangle, \tag{37}$$

$$-c^{\dagger}_{U\sigma}c_{i\sigma}(c^{\dagger}_{L\alpha}c^{\dagger}_{i\beta})|0\rangle = \left(-\frac{\mathrm{i}}{\sqrt{2}}\sigma^{y}_{\alpha\beta}s^{\dagger}_{LU} + \frac{\mathrm{i}}{\sqrt{2}}[\sigma^{y}\sigma]_{\alpha\beta}\mathbf{t}^{\dagger}_{LU}\right)|0\rangle. \tag{38}$$

In the analysis of contributions from quantum fluctuations in the ground state of the system to the spectral function the following formulae are useful:

$$\mathbf{S}_L\mathbf{S}_i(s^{\dagger}_{LU}c^{\dagger}_{i\beta}|\phi\rangle = \tfrac{1}{2}\sigma_{\alpha\beta}(\mathbf{t}^{\dagger}_{LU}c^{\dagger}_{i\alpha})|0\rangle, \tag{39}$$

$$\mathbf{S}_U\mathbf{S}_i(s^{\dagger}_{LU}c^{\dagger}_{i\beta}|\phi\rangle = -\tfrac{1}{2}\sigma_{\alpha\beta}(\mathbf{t}^{\dagger}_{LU}c^{\dagger}_{i\alpha})|0\rangle. \tag{40}$$

References

[1] Tranquada J M 2005 *Preprint* cond-mat/0512115 and references therein

[2] Thurston T R, Birgeneau R J, Kastner M A, Preyer N W, Shirane G, Fujii Y, Yamada K, Endoh Y, Kakurai K, Matsuda M, Hidaka Y and Murakami T 1989 *Phys. Rev.* B **40** 4585
Cheong S-W, Aeppli G, Mason T E, Mook H, Hyden S M, Canfield P C, Fisk Z, Clausen K N and Martinez J L 1991 *Phys. Rev. Lett.* **67** 1791
Thurston T R, Gehring P M, Shirane G, Birgeneau R J, Kastner M A, Endoh Y, Matsuda M, Yamada K, Kojima K and Tanaka I 1992 *Phys. Rev.* B **46** 9128

[3] Tranquada J M, Sternlieb B J, Axe J D, Nakamura Y and Uchida S 1995 *Nature* **375** 561

[4] Matsuda M, Birgeneau R J, Chou H, Endoh Y, Kastner M A, Kojima H, Kuroda K, Shirane G, Tanaka I and Yamada K 1993 *J. Phys. Soc. Japan* **62** 443
Yamada K, Wakimoto S, Shirane G, Lee C H, Kastner M A, Hosoya S, Greven M, Endoh Y and Birgeneau R J 1995 *Phys. Rev. Lett.* **75** 1626
Hirota K, Yamada K, Tanaka I and Kojima H 1998 *Physica* B **241–243** 817
Kimura H, Hirota K, Matsushita H, Yamada K and Endoh Y 1999 *Phys. Rev.* B **59** 6517
Tranquada J M, Ichikawa N, Kakurai K and Uchida S 1999 *J. Phys. Chem. Solids* **60** 1019
Tranquada J M, Ichikawa N and Uchida S 1999 *Phys. Rev.* B **59** 14712

[5] Kivelson S A, Bindloss I P, Fradkin E, Oganesyan V, Tranquada J M, Kapitulnik A and Howald C 2003 *Rev. Mod. Phys.* **75** 1201 and references therein

[6] Ando Y, Segawa K, Komiya S and Lavrov A N 2002 *Phys. Rev. Lett.* **88** 137005

[7] Hess C, Büchner B, Hücker M, Gross R and Cheong S-W 1999 *Phys. Rev.* B **59** 10397

[8] Hunt A W, Singer P M, Thurber K R and Imai T 1999 *Phys. Rev. Lett.* **82** 4300
Julien M-H, Borsa F, Carreta P, Horvatič M, Berthier C and Lin C T 1999 *Phys. Rev. Lett.* **83** 604
Singer P M, Hunt A W, Cederström A F and Imai T 1999 *Phys. Rev.* B **60** 15345
Suh B J, Hammel P C, Hücker M and Büchner B 1999 *Phys. Rev.* B **59** R3952
Curro N J, Hammel P C, Suh B J, Hücker M, Büchner B, Ammerahl A and Revcolevschi A 2000 *Phys. Rev. Lett.* **85** 642
Suh B J, Hammel P C, Hücker M, Büchner B, Ammerahl U and Revcolevschi A 2000 *Phys. Rev.* B **61** R9265
Teitel'baum G B, Büchner B and de Gronckel H 2000 *Phys. Rev. Lett.* **84** 2949
Hunt A W, Singer P M, Cederström A F and Imai T 2001 *Phys. Rev.* B **64** 134525
Julien H-H, Campana A, Rigamonti A, Carretta P, Borsa F, Kuhns P, Reyes A P, Moulton W G, Horvatič M, Berthier C, Vietkin A and Revcolevschi A 2001 *Phys. Rev.* B **63** 144508
Teitel'baum G B, Abu-Shiekah I M, Bakharev O, Brom H B and Zaanen J 2001 *Phys. Rev.* B **63** 020507
Simovič B, Hammel P C, Hücker M, Büchner B and Revcolevschi A 2003 *Phys. Rev.* B **68** 012415

[9] Božin E S, Kwei G H, Takagi H and Billinge S J L 2000 *Phys. Rev. Lett.* **84** 5856
[10] Braden M, Meven M, Reichardt W, Pintschovius L, Fernandez-Diaz M T, Heger G, Nakamura F and Fujita T 2001 *Phys. Rev.* B **63** 140510
[11] Bianconi A, Saini N L, Lanzara A, Missori M, Oyanagi T R H, Yamaguchi H, Oka K and Ito T 1996 *Phys. Rev. Lett.* **76** 3412
Lanzara A, Saini N L, Rossetti T, Bianconi A, Oyanagi H, Yamaguchi H and Maeno Y 1996 *Solid State Commun.* **97** 93
Saini N L, Lanzara A, Oyanagi H, Yamaguchi H, Oka K, Ito T and Bianconi A 1997 *Phys. Rev.* B **55** 12759
[12] Fedorov A V, Valla T, Johnson P D, Li Q, Gu G D and Koshizuka N 1999 *Phys. Rev. Lett.* **82** 2179
Ino A, Kim C, Mizokawa T, Shen Z-X, Fujimori A, Takaba M, Tamasaku K, Eisaki H and Uchida S 1999 *J. Phys. Soc. Japan* **68** 1496
Valla T, Fedorov A V, Johnson P D, Wells B O, Hulbert S L, Li Q, Gu G D and Koshizuka N 1999 *Science* **285** 2110
[13] Zhou X J, Bogdanov P, Kellar S A, Noda T, Eisaki H, Uchida S, Hussain Z and Shen Z-X 1999 *Science* **286** 268
[14] Zhou X J, Yoshida T, Kellar S A, Bogdanov P V, Lu E D, Lanzara A, Nakamura M, Noda T, Kakeshita T, Eisaki H, Uchida S, Fujimori A, Hussain Z and Shen Z-X 2001 *Phys. Rev. Lett.* **86** 5578
[15] Campuzano J C, Norman M R and Randeria M 2003 *The Physics of Conventional and Unconventional Superconductors* ed K H Bennemann and J B Ketterson (Berlin: Springer)
[16] Damascelli A, Hussain A Z and Shen Z-X 2003 *Rev. Mod. Phys.* **75** 473
[17] Ichioka M and Machida K 1999 *J. Phys. Soc. Japan* **68** 4020
[18] Fleck M, Lichtenstein A I, Pavarini E and Oleś A M 2000 *Phys. Rev. Lett.* **84** 4962
Fleck M, Lichtenstein A I and Oleś A M 2001 *Phys. Rev.* B **64** 134528
[19] Markiewicz R S 2000 *Phys. Rev.* B **62** 1252
Wróbel P and Eder R 2000 *Phys. Rev.* B **62** 4048
[20] Wróbel P and Eder R 2000 *Int. J. Mod. Phys.* B **14** 3759
[21] Zacher M G, Eder R, Arrigoni E E and Hanke W 2000 *Phys. Rev. Lett.* **85** 2585
[22] Carlson E W, Orgad D, Kivelson S A and Emery V J 2001 *Phys. Rev.* B **62** 3422
[23] Eroles J, Ortiz G, Balatsky A V and Bishop A R 2001 *Phys. Rev.* B **64** 174510
[24] Granath M, Oganesyan V, Kivelson S A, Fradkin E and Emery V J 2001 *Phys. Rev. Lett.* **87** 167011
Gweon G-H, Denlinger J D, Allen J W, Claesson R, Olson C G, Hoechst H, Marcus J, Schlenker C and Schneemeyer L F 2001 *J. Electron Spectrosc. Relat. Phenom.* **117/118** 481
Orgad D, Kivelson S A, Carlson E W, Emery V J, Zhou X J and Shen Z-X 2001 *Phys. Rev. Lett.* **86** 4362
[25] Granath M, Oganesyan V, Orgad D and Kivelson S A 2002 *Phys. Rev.* B **65** 184501
[26] Zacher M G, Eder R, Arrigoni E E and Hanke W 2002 *Phys. Rev.* B **65** 045109
[27] Carlson E W, Emery V J, Kivelson S A and Orgad D 2003 *The Physics of Conventional and Unconventional Superconductors* ed K H Bennemann and J B Ketterson (Berlin: Springer)
Granath M 2004 *Preprint* cond-mat/0401063
[28] Ino A, Kim C, Nakamura M, Yoshida T, Mizokawa T, Fujimori A, Kakeshita T, Eisaki H and Uchida S 2000 *Phys. Rev.* B **62** 4137
[29] Salkola M I, Emery V J and Kivelson S A 1996 *Phys. Rev. Lett.* **77** 155
[30] Anderson P W 1987 *Science* **235** 1196
Rokshar D S and Kivelson S A 1988 *Phys. Rev. Lett.* **61** 2376
Dombre T and Kotliar G 1989 *Phys. Rev.* B **39** 855
Fradkin E and Kivelson S A 1990 *Mod. Phys. Lett.* B **4** 225
Read N and Sachdev S 1990 *Phys. Rev.* B **42** 4568
Sachdev S and Read N 1996 *Phys. Rev. Lett.* **77** 4800
Read N and Sachdev S 1998 *Nucl. Phys.* B **316** 609
Vojta M and Sachdev S 1999 *Phys. Rev. Lett.* **83** 3916
Altman E and Auerbach A 2002 *Phys. Rev.* B **65** 104508
Sachdev S and Park K 2002 *Ann. Phys.* **298** 58
Vojta M 2002 *Phys. Rev.* B **66** 104505
Sachdev S 2003 *Rev. Mod. Phys.* **75** 913
[31] Eder R and Ohta Y 2004 *Phys. Rev.* B **69** 094433
[32] Eder R and Ohta Y 2004 *Phys. Rev.* B **69** 100502(R)
[33] Hayden S M, Mook H A, Dai P, Perring T G and Doğan F 2004 *Nature* **429** 531
Tranquada J M, Woo H, Perring T G, Goka H, Gu G D, Xu G, Fujita M and Yamada K 2004 *Nature* **429** 534
[34] Wróbel P, Maciąg A and Eder R 2006 *J. Phys.: Condens. Matter* **18** 1249
[35] Chernyshev A L, Castro Neto A H and Bishop A R 2000 *Phys. Rev. Lett.* **84** 4922

Chernyshev A L, White S R and Castro Neto A H 2002 *Phys. Rev.* B **65** 214527
[36] Oleś A M 2000 *Acta Phys. Pol.* B **31** 2963
Góra D, Rościszewski K and Oleś A M 1999 *Phys. Rev.* B **60** 7429
Rościszewski K and Oleś A M 2003 *J. Phys.: Condens. Matter* **15** 8363
Raczkowski M, Frésard R and Oleś A M 2006 *Phys. Rev.* B **73** 174525
[37] Becker K W, Eder R and Won H 1992 *Phys. Rev.* B **45** 4864
[38] Eder R 1998 *Phys. Rev.* B **57** 12832
[39] Jurecka C and Brenig W 2000 *Phys. Rev.* B **61** 14307
Brenig W and Becker K W 2001 *Phys. Rev.* B **64** 214413
Hess C, Baumann C, Ammerahl U, Büchner B, Heidrich-Meisner F, Brenig W and Revcolevschi A 2001 *Phys. Rev.* B **64** 184305
Jurecka C and Brenig W 2001 *Phys. Rev.* B **63** 094409
Heidrich-Meisner F, Honecker A, Cabra D C and Brenig W 2003 *Phys. Rev.* B **68** 134436
[40] Chernyshev A L and Wood R F 2003 *Models and Methods of High-T_c Superconductivity: Some Frontal Aspects* vol 1, ed J K Srivastava and S M Rao (Hauppauge, NY: Nova Science Publishers, Inc.) and references therein
[41] Bulaevskii L N, Nagaev E L and Khomskii D I 1968 *Zh. Eksp. Teor. Fiz.* **54** 1562
Brinkman W F and Rice T M 1970 *Phys. Rev.* B **2** 1324
Kane C L, Lee P A and Read N 1988 *Phys. Rev.* B **39** 6880
Marsiglio F, Ruckenstein A E, Schmitt-Rink S and Varma C M 1991 *Phys. Rev.* B **43** 10882
Schmitt-Rink S, Varma C M and Ruckenstein A E 1988 *Phys. Rev. Lett.* **60** 2793
Shraiman B and Siggia E 1988 *Phys. Rev. Lett.* **60** 740
Trugman S 1988 *Phys. Rev.* B **37** 1597
Trugman S 1990 *Phys. Rev.* B **41** 892
See also Schrieffer J R, Wen X-G and Zhang S-C 1988 *Phys. Rev. Lett.* **60** 944
Béran P, Poilblanc D and Laughlin R B 1996 *Nucl. Phys.* B **473** 707
Laughlin R B 1997 *Phys. Rev. Lett.* **79** 1726
[42] Ino A, Kim C, Nakamura M, Yoshida T, Mizokawa T, Fujimori A, Shen Z-X, Kakeshita T, Eisaki H and Uchida S 2002 *Phys. Rev.* B **65** 094504
[43] Eder R and Becker K W 1991 *Phys. Rev.* B **44** 6982
Eder R and Becker K W 1990 *Z. Phys.* B **78** 219
Eder R, Becker K W and Stephan W 1990 *Z. Phys.* B **81** 33
[44] Nazarenko A *et al* 1995 *Phys. Rev.* B **51** 8676
[45] Kyung B and Ferrell R A 1996 *Phys. Rev.* B **54** 10125
[46] Xiang T and Wheatley J M 1996 *Phys. Rev.* B **54** R12653
[47] Belinicher V I *et al* 1996 *Phys. Rev.* B **54** 14914
[48] Eder R *et al* 1997 *Phys. Rev.* B **55** R3414
[49] Lee T K and Shih C T 1997 *Phys. Rev.* B **55** 5983
[50] Kim C *et al* 1998 *Phys. Rev. Lett.* **80** 4245
[51] Tohyama T, Nagai S, Shibata Y and Maekawa S 1999 *Phys. Rev. Lett.* **82** 4910
Tohyama T and Maekawa S 2000 *Supercond. Sci. Technol.* **13** R17
[52] Wells B O, Shen Z-X, Matsuura A, King D M, Kastner M A, Greven M and Birgeneau R J 1995 *Phys. Rev. Lett.* **74** 964
[53] Bansil A, Lindroos M, Sahrakorpi S and Markiewicz R S 2005 *Phys. Rev.* B **71** 012503
[54] Wróbel P 2006 *Phys. Rev.* B **74** 014507
[55] Niemöller T, Büchner B, Cramm M, Huhnt C, Tröger L and Tischer M 1998 *Physica* C **299** 191